# *THERMAL CHARACTERISTICS OF NATURAL ESTER TRANSFORMERS UNDER EXTREME AMBIENT TEMPERATURES*

***DaWei FENG [1*], TingTing LIU [1], Zhe LI [1], YongJian LI, and JiLiang YI [2]***

[*1] Key Laboratory of Electromagnetic Field and Electrical Apparatus Reliability of Hebei Province, School of Electrical Engineering, Hebei University of Technology, Tianjin, China

[2] SUNTEN Electrical Equipment Co., Ltd, Foshan, China

[*] Corresponding author; E-mail: josaturday@hebut.edu.cn

*With growing environmental concerns, natural ester transformers are widely used due to their excellent properties and good biodegradability. However, their thermal characteristics under extreme ambient temperatures remain unclear, limiting their widespread adoption. Herein, a Numerical simulation model is used to simulate and evaluate the temperature distribution, hot-spot temperature and thermal stability of natural ester transformers. A mineral oil transformer is used for comparison. The results indicate that the hot-spot temperature of the natural ester transformer is always higher than that of the mineral oil transformer under the same heat dissipation structure. With the increase of ambient temperature, the variation trends of their hot-spot temperatures initially decrease and then increase, and the minimum hot-spot temperatures appear around the -10 °C ambient temperature. The hot-spot temperature increases when ambient temperature continues to go up. However, the hot-spot temperature of the natural ester transformer remains within the limits specified by the IEEE standard under the extremely high ambient temperature (52.2°C). In contrast, the mineral oil transformer exhibits localized overheating in the windings, in which the overheated zone accounts for approximately 50% of the total winding. Actually, when the ambient temperature exceeds 45°C, the hot-spot temperature of the mineral oil transformer reaches its limit, while that of the natural ester transformer remains within its safe limit. The results demonstrate the superiority of natural ester transformers when used at high ambient temperatures, while also providing a reference for the design and application of natural ester transformers under extreme ambient temperatures.*

Key words: *Transformer, Natural esters, Thermal characteristics, extreme ambient temperature*

## 1. Introduction

oil-immersed transformers are the core equipment of voltage conversion and energy transmission in the power system, whose main insulation consists of oil-paper insulation [1][2]. Traditional mineral oils are derived from petroleum fractionation and have the advantages of low viscosity, low pour point and good electrical properties. However, the increasing requirements for environmental protection and fire prevention in recent years have made the disadvantages of mineral oils, such as poor biodegradability and low ignition point, increasingly prominent [3]. To address this issue, natural esters derived from plant seeds have become a research hotspot due to their high flash point, high fire point and good biodegradability [4]. With the development of environmental protection requirements, the application of natural ester transformers will become increasingly common, especially in areas that are prone to pollution, such as water sources, underground areas, and oceans. With the increasing demand for natural ester transformers, traditional mineral oil transformer factories have begun to manufacture natural ester transformers. However, the impact of insulation oils with different viscosity-temperature characteristics on the temperature field distribution is unknown, especially the lack of results at extreme ambient temperatures, which poses a challenge for designers.

The use of multi-physics simulation can quickly obtain the temperature field distribution of transformers and optimize their heat dissipation structure. For example, Numerical simulation with solvers and algorithms library simulates heat transfer and flow processes in the transformer with high accuracy [5][6]. IEEE Std C57.91 and IEC 60076-7 stipulate that the hot-spot temperature and thermal deterioration of the windings are only considered for the distribution transformer operating under rated load; The relative aging rate of insulation paper is also based on the hot-spot temperature of the windings. Therefore, the hot-spot temperature of the distribution transformer can reflect its overall performance [7][8]. Many scholars have conducted CFD simulations of the temperature field distribution of transformers based on two-dimensional or three-dimensional models. B. Melka et al. calculated and compared the cooling efficiency of mineral, synthetic, and natural ester oils, and found that the synthetic ester has a better cooling effect than mineral oil at maximum ambient temperature of 30 °C [9]. Deng et al. combined fluid-thermal field calculation with the machine learning model to predict the hot-spot temperature of transformers, whose predicted results are consistent with the experimental and simulation data [10]. Feng et al. established a three-dimensional model to calculate the oil flow distribution, temperature distribution, and the location of the hot-spot temperatures within the transformer [11]. In addition, N. C. Chereches et al. conducted the steady-state numerical study on the transformer and optimized its internal cooling structure based on the thermal-fluid field results [12]. Zhang et al. investigated the influence patterns of winding thermal defects on the temperature of local areas with the CFD model, and found that the temperature rise of the oil in the oil channel increases linearly with the overheat temperature [13].

The flow and heat dissipation performance of insulating oil depends on oil temperature, which is affected by ambient temperature, and the ambient temperature also affects the heat exchange with the outside of the transformers. However, research on the temperature field distribution of natural ester transformers at different ambient temperatures is limited, especially at extreme temperatures. Therefore, temperature characteristics of natural ester transformers under extreme ambient temperature were studied with a three-dimensional symmetry model, which provides a reference for the design and application of natural ester transformers in extreme ambient temperatures conditions.

## 2. Model building and setup

### 2.1. Model building

To improve the computational efficiency and accuracy, two models were used in this study:

1)The geometry model suitable for meshing was developed.

2)The shell conduction model simulating heat conduction in the oil tank was set.

Existing word has shown that the size of the problem grows with the square of the nodes' number and the computation time grows with the cube of the nodes' number [14]. Therefore, to focus limited computing resources on the key point of the problem, the transformer's geometry model was appropriately simplified. The transformer structures that mainly affect hot-spot temperature, such as core, windings, oil tank and cooling fins, were retained, while the clamping structure of the core and the metallic fittings outside the oil tank were neglected. The geometry model and the mesh model were shown in Figure 1. Geometry model of the transformer and Figure 2. Figure 3 illustrated the winding structure of the transformer, and windings and oil channels were numbered.

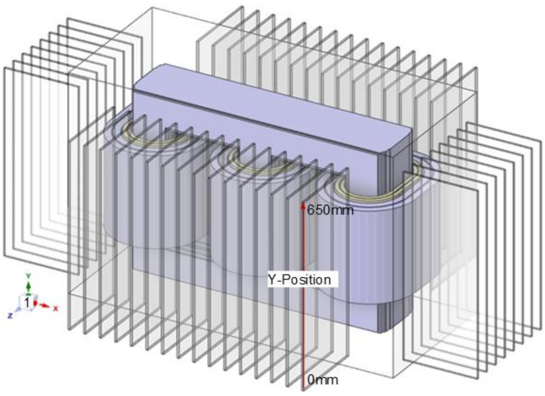


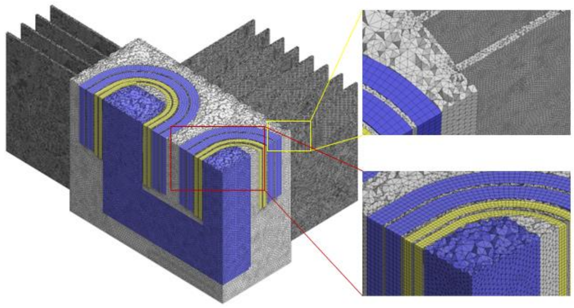

**Figure 1. Geometry model of the transformer** **Figure 2. Mesh model of the transformer**

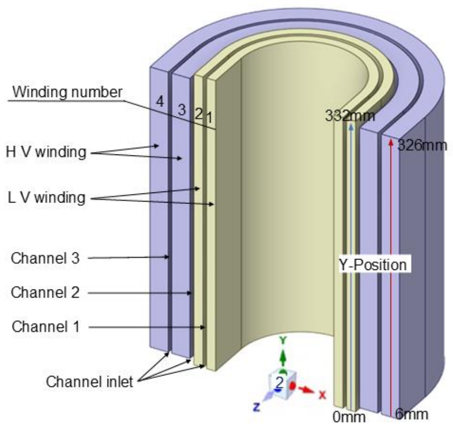


**Figure 3. Winding structure of the transformer**

It has been verified that adding the extremely thin oil tank zone to the exterior of the transformer's geometry model causes an exponential increase in the number of mesh cells. This situation is also more likely to produce pc e of the calculations. There are two solutions to this other is to use shell conduction model. However, the late heat conduction along the normal direction of the odel can simulate heat conduction along both the nor ll, which aligns more closely with the actual situati used to simulate heat conduction within the oil tank.

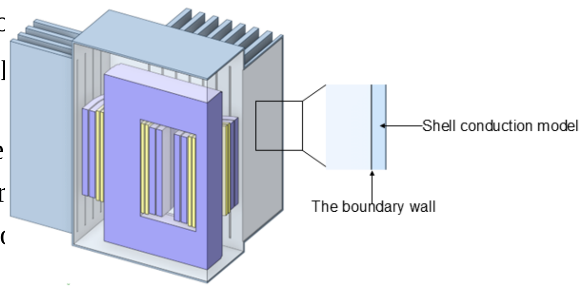

Figure 4.Boundary wall with shell conduction model illustrates the boundary wall with shell conduction model.

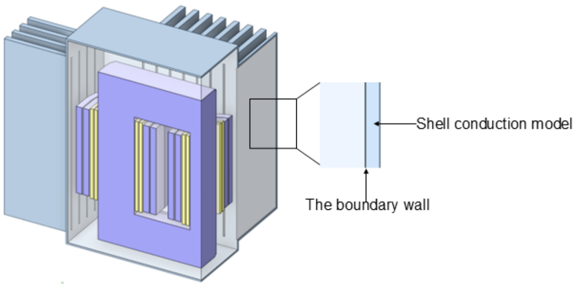


**Figure 4.Boundary wall with shell conduction model**

### 2.2. Thermal properties of transformer oils

For comparison, mineral oil (Karamay 25#) and natural ester (FR3) were used for simulation calculations. Their thermal properties were shown in Table 1, where *T* stands for the thermodynamic temperature. Parameters of the two insulation oils were obtained based on laboratory measurements and the manufacturer's specifications [15][16].

**Table 1**. **Thermal properties of mineral oil (karamay 25#) and natural ester (FR3)**

| Properties | Natural ester | Mineral oil |
|---|---|---|
| **Density ($kg\ m^{-3}$)** | 1132-0.7243T | 1098.72-0.712T |
| **Specific heat ($J\ kg^{-1}\ K^{-1}$)** | 802.26+3.25T | 807.163+3.58T |
| **Thermal conductivity ($W\ m^{-1}\ K^{-1}$)** | $0.1953-7.969\times10^{-5}T$ | $0.1509-7.101\times10^{-5}T$ |
| **Viscosity ($kg\ m^{-1}\ s^{-1}$)** | 0.00749+0.226exp(-(T-252.83)/1.4)+ 0.434exp(-(T-52.83)/21.66) | 0.0029+77412.69exp(-T/18.95)+ $2.44\times10^{15}$exp(-T/6.96) |

### 2.3. Selection of typical ambient temperatures

The pour point of insulating oils is the lowest temperature at which they can flow [17]. Therefore, if the ambient temperature is lower than the pour point of transformer oils, condensation of the transformer oil may occur in the zones away from the heat generation zones, such as the bottom of the oil tank and cooling fins. Considering that the pour point of FR3 natural esters is about -21 ℃, the extremely low ambient temperature is set at -20 °C although mineral oil has a lower pour point. Based on the historical highest temperature in China, the extremely high ambient temperature is set at 52.2 °C, which is also close to the world's highest ambient temperature. Table 2 lists six typical ambient temperatures.

**Table 2. Typical ambient temperatures**

| Ambient temperature | Introduction |
|---|---|
| -20℃ | The extremely low ambient temperature |
| -10℃ | Ambient temperature in winter |
| 0℃ | |
| 22℃ | Temperature during the temperature rise test of the transformer |

| | |
|---|---|
| 40℃ | Surface temperature in summer |
| 52.2℃ | The extremely high ambient temperature |

### 2.4. Simulation settings

The geometry model of the transformer was divided into four parts, one of which was selected for calculations. Symmetric boundary conditions were applied to the symmetry plane. A shell conduction model with 1.2 mm steel was applied on the exterior surface of the oil zone, and temperature boundary conditions were applied to the exterior surface of the shell conduction model. By setting the above boundary conditions, the number of mesh cells was greatly reduced.

In this simulation, the laminar model was chosen according to the calculation of the Reynolds number and the existing references [18]-[21]. The insulating oil with a low velocity in transformers was regarded as an incompressible fluid. Therefore, a pressure-based solver was employed. To ensure computational stability, the time step was automatically controlled by the software, and the coupled algorithm was used for the coupling of pressure and velocity. Additionally, Body Force Weighted or PRESTO! can be chosen as the pressure discretization method for natural flow induced by gravity.

## 3. Model verifications

### 3.1. Mesh independence verification

In numerical calculations, the discrete equations are solved after discretization of the differential equations, which will introduce discretization error. With the decline of the cell size, the discretization errors continuously decrease; thus, the solution of the discretized equations gradually approximates the solution of the original differential equations. Therefore, to determine the minimum number of cells required for accurate results, eight sets of calculations were conducted using an overall and then locally refined mesh method when the ambient temperature was 22℃. The number of cells and the changes in hot-spot temperatures with increase of the cells number are shown in Figure 5. The hot-spot temperature of the transformer calculated by Mesh 5 in this figure shows a significant decrease. Based on Mesh 4, the narrow regions, such as oil channels and cooling fins, are locally refined in Mesh 5; thus, the discretization errors are significantly reduced, making the numerical solution close to the true solution. The result of continuing to increase the number of cells also confirms this point. When the number of cells is 12,242,582-17,304,804, the hot-spot temperature of the transformer remained almost unchanged. Consequently, Mesh 5 was ultimately adopted for subsequent calculations. The hot-spot temperature of the transformer calculated with Mesh 5 is 77.3 °C while that obtained by temperature rise experiment is 77 °C, which shows a 0.3 °C error and verifies the accuracy of the model.

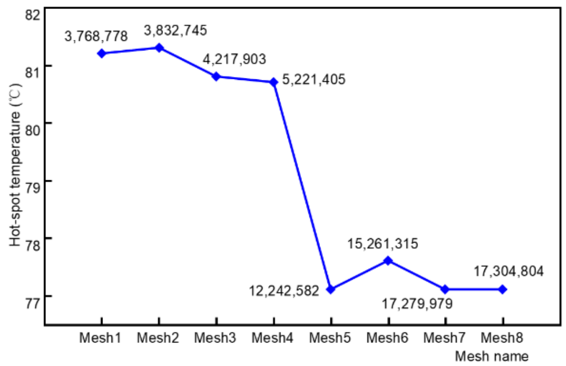


**Figure 5. Changes in hot-spot temperatures with increase of the cells number**

## 4. Results

### 4.1. Transformer temperature profiles

To compare the effect of oil viscosity on the temperature field in the transformer, the calculations were conducted using the same transformer structure. Under the same legend, the temperature profiles of the transformer filled with the mineral oil (TFMO) and the transformer filled with the natural ester (TFNE) under different ambient temperatures are shown in TFNE is more prone to forming localized high temperature in the winding, core and upper part of the oil tank compared to TFMO. For example, the localized high temperature around the upper windings in TFNE is more obvious below 0 ℃.

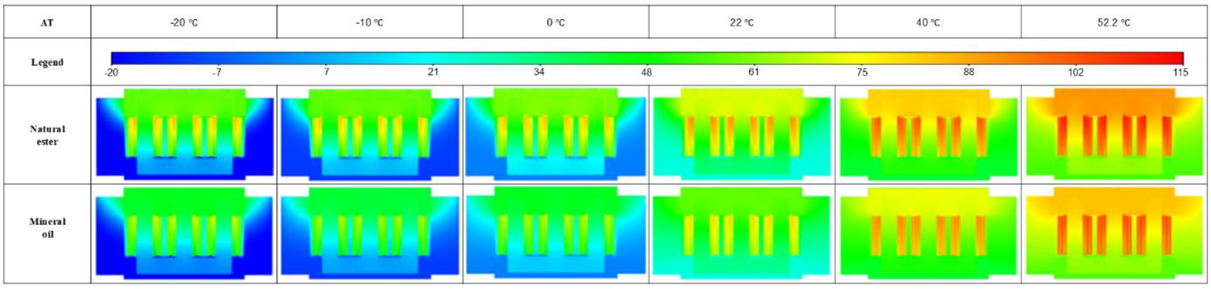


Figure 6, where *AT* stands for ambient temperature. TFNE is more prone to forming localized high temperature in the winding, core and upper part of the oil tank compared to TFMO. For example, the localized high temperature around the upper windings in TFNE is more obvious below 0 ℃.

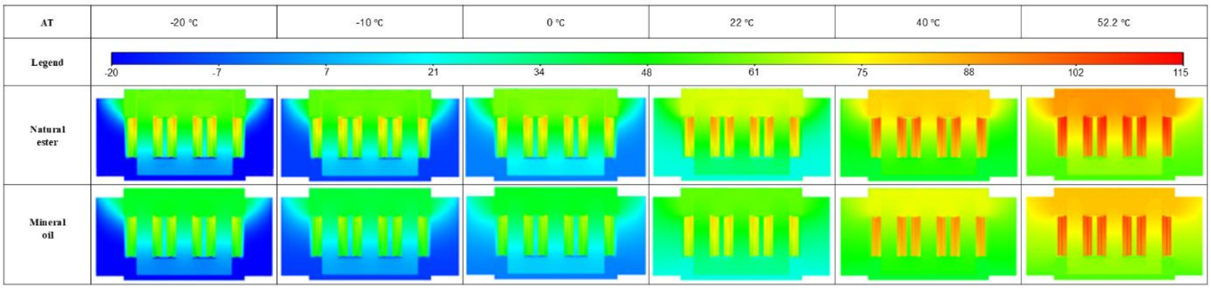


**Figure 6. Temperature profiles of TFMO and TFNE at different ambient temperatures**

To explain this phenomenon, the oils velocity of three positions in the cooling fins and Channel1 are presented in Figure 7. Y-Position represents the vertical distance measured upward from the bottom of Channel 1 and cooling fins. High viscosity of natural ester decreases fluidity; thus, the heat generated by the windings cannot be carried away inefficiently, which leads to a localized temperature increase in the windings. For natural oil circulation transformers, expanding the oil channel may be a solution to reduce winding temperature rise when filled with natural esters.

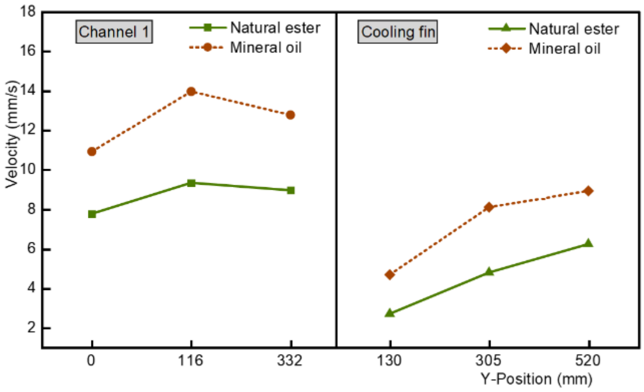


**Figure 7. Velocity of the natural ester and mineral oil in the Cooling fin and Channel1**

### 4.2. Temperature rises at the top of the windings

The top winding temperature rises of TFNE and TFMO at different ambient temperatures are calculated, and the specific data are shown in Figure 8. Herein, winding temperature rise represents the difference between the winding temperature and the ambient temperature.

With the increase of ambient temperatures, top winding temperature rises of TFNE and TFMO initially increase and then decrease. The temperature rise of the windings of TFNE and TFMO reaches their maximum values of 81.9 °C and 66.2 °C at 0 °C, respectively. This phenomenon is caused by the synergistic effect of the flow and heat dissipation of oils. Although the insulation oil is heated by the winding, the temperature of the insulation oil in the cooling fins mainly depends on the ambient temperature. When the temperature is below 0 °C, the viscosity of the insulation oil is very high and its flow is slow, leading to a rarely heat dissipation effect of the cooling fins. At the same time, the thermal conductivity of insulating oil also decreases with the increment of temperature. Therefore, the temperature rise of the winding increases with the increment of ambient temperature. When the temperature exceeds 0 °C, the viscosity of the oil decreases significantly with increasing temperature, which improves the heat dissipation effect of insulating oil. As a result, the increase rate of winding temperature is slower than the increase rate of ambient temperature, leading to gradual decline of the temperature rise of windings.

For different oil, the temperature rise difference reaches the maximum value of 15.7 °C at 0 °C. Similarly, when the ambient temperature is 0 °C, the viscosity difference between natural ester and mineral oil also reaches their maximum value. To investigate whether there is a correlation between the viscosity difference (natural esters and mineral oils) and the temperature rise difference (the windings of TFNE and TFMO), corresponding data are calculated and shown in Figure 9. The viscosity difference and the temperature rise difference have a same variation trend, and their maximum values occur at the same ambient temperature. Meaningfully, this correlation between the viscosity difference and the temperature rise difference can be used to predict the winding temperature rise trend when a new insulating oil is used in the same structure.

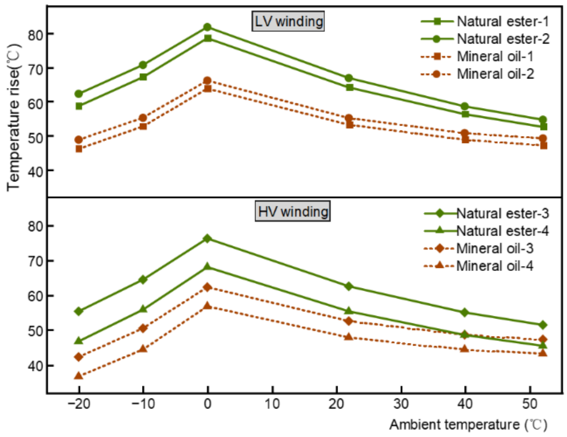


**Figure 8. Top windings temperature rises of TFNE and TFMO**

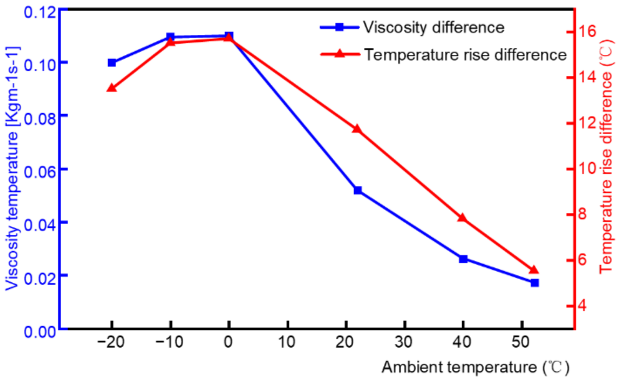


**Figure 9. Difference in oil viscosity and winding temperature rise at different ambient temperatures**

### 4.3. Thermal performance of transformers at 52.2 ℃

Under extremely high ambient temperature (52.2 °C), the hot-spot temperatures of TFMO and TFNE are 101.4 °C and 106.9 °C, respectively. IEEE Std C57.154 and IEC 60076-14 stipulate the maximum temperature limitation for insulation paper in oil-immersed transformers, and the specific values are shown in Table 3 [22]-[25]. Although TFNE exhibits the localized high temperature in the windings, its hot-spot temperature (106.9 °C) does not exceed the temperature limit of 110 °C. However, TFMO's maximum temperature (101.4 °C) exceeds the temperature limit of 95 °C by 6.4 °C, which does not meet the operational requirements. The overheated zone is shown in Figure 10, in which the grey and colored zones represent areas above 95°C, and the yellow zone represents the geometry model of the windings. Figure 10 shows that the overheated zone is mainly concentrated in the upper part of the windings, accounting for approximately 50% of the total windings. Here, Winding 3 has the most overheated area (>95°C), followed by Winding 2, while Winding 2 has the highest overheating temperature. Winding 4 is located at the outermost side, which has a higher heat exchange efficiency with the insulating oil, resulting in the smallest overheating area. This conclusion indicates the superiority of natural ester insulating oil when used at high temperatures. If only considering temperature limitations, mineral oil transformers can be directly replaced with natural esters without change of the heat dissipation structure, and the natural ester transformer after replacement have a higher temperature rise but meet standard requirements.

**Table 3. The hot-spot temperature that oil-immersed paper can withstand**

| Insulation paper | Insulating oil | Temperature limits |
|---|---|---|
| Common insulating paper | Mineral oil | 95 °C |
| | Natural ester | 110 °C |
| Thermally upgraded paper | Mineral oil | 110 °C |
| | Natural ester | 130 °C |

To determine the axial position of the hot-spot temperature, the temperature changes along the axial direction of Winding 2 were calculated, and the results are shown in Figure 11. Y-Position represents the vertical distance measured upward from the bottom of Winding 2. The oil difference leads to the difference in the winding temperatures along axial height. However, the Y-Position of the hot-spot temperature remains unchanged, which occurs at about 97 % (321 mm) of the upper part of the winding. It is worth noting that the winding temperatures of TFMO and TFNE overlap at 31% (103mm) of the winding, and the winding temperatures above and below this position show opposite results.

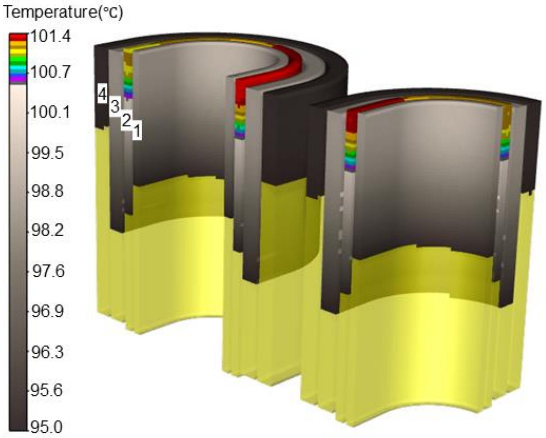


**Figure 10. The overheated zone and the value near the hot-spot temperature**

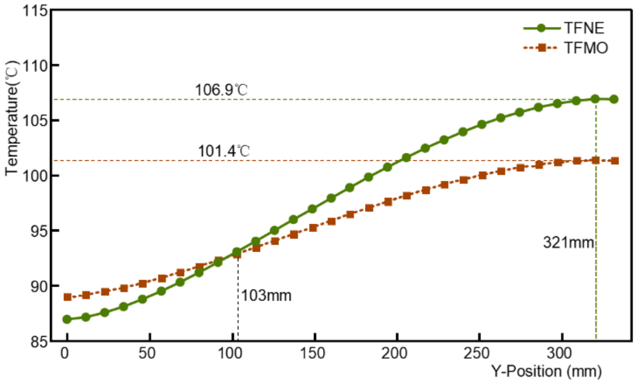


**Figure 11. Temperature variations along the axial direction of Winding 2**

To explain the phenomenon, the temperature, velocity and thermal conductivity of the oils at the inlet of Channel 1 are calculated, as shown in Table 4. The oil temperatures at the inlet of the oil Channel 1 are nearly the same for the two oils. Since the thermal conductivity of the natural ester is slightly higher than that of the mineral oil, leading to a higher cooling efficiency on the windings. Thus, the winding temperature of TFNE is lower than that of TFMO at the bottom of the winding. The temperature of transformer oils increases after absorbing the heat generated by the windings, resulting in a decrease in density, which drives an upward flow of transformer oils. Figure 12 shows that the temperature of natural ester is consistently higher than that of mineral oil in the upper part of Channel 1, which reduces the temperature difference between the winding and the natural esters, leading to a decrease in the heat dissipation effect on the winding. Therefore, the temperature of the upper winding in TFNE is higher than that in TFMO.

**Table 4. The temperature, velocity and thermal conductivity of the oils at the inlet of Channel1**

| Channel 1 | Natural ester | Mineral oil |
|---|---|---|
| Inlet temperature [℃] | 61.5 | 61.7 |
| Inlet velocity[mm/s] | 11 | 14.8 |
| Thermal conductivity (61 ℃) [$Wm^{-1}K^{-1}$] | 0.17 | 0.13 |

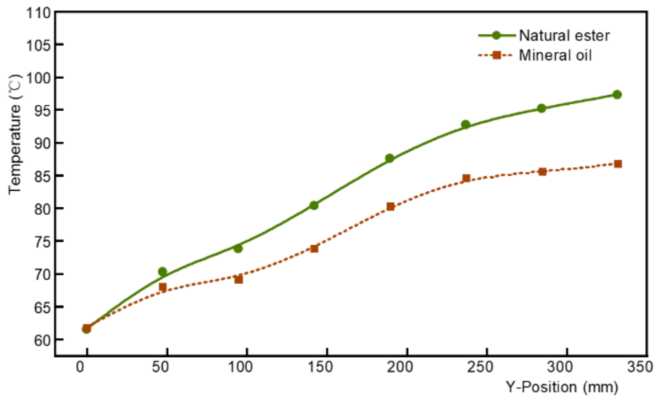


**Figure 12. Temperature variations along the axial direction of Channel1**

### 4.4. The hot-spot temperature at difference ambient temperature

The hot-spot temperatures of the transformers at all the ambient temperatures were calculated, as shown in Figure 13. The hot-spot temperatures of TFNE are always higher than those of TFMO at all ambient temperatures, and the variation trends firstly decrease and then increase. When the ambient temperature is -10 °C, the hot-spot temperatures of TFNE and TFMO reach the minimum values, i.e., 80.9 °C and 65.4 °C, respectively. When the temperature is below -10 °C, the hot spot temperature will actually increase, mainly due to the significant increase in viscosity at low temperatures.

When the ambient temperature exceeds 45 °C, TFMO exceeds the temperature limit specified in IEC standard 60076, which indicates that the maximum operating ambient temperature for this mineral oil is 45 °C. Whereas the hot-spot temperature of TFNE does not exceed the temperature limits even at 52.2 °C ambient temperature, which confirms the feasibility of using natural esters at high ambient temperatures.

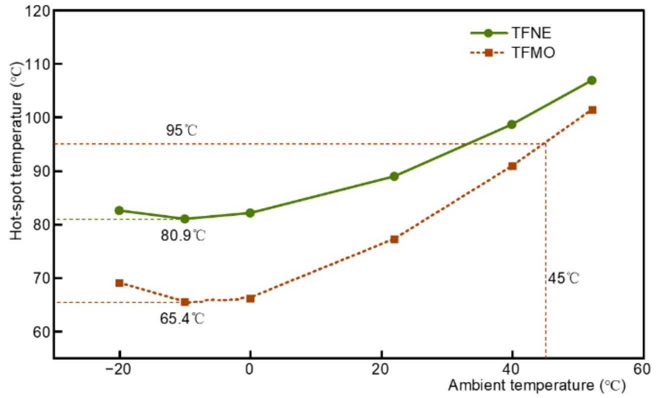


**Figure 13. Hot-spot temperatures of TFMO and TFNE at difference ambient temperature**

### 4.5. Reflections on the potential risks of natural ester transformers at high temperatures

With the same heat dissipation structure, the temperature rise of TFNE is higher. Meanwhile, the hot-spot temperature is approximately 4.5 °C higher than that of TFMO under extreme high-temperature (52.2 °C). Existing research indicates that natural esters can decrease the aging rate of insulation paper, so the slight increase in temperature can hardly affect the thermal aging life of insulation paper immersed in natural esters [26]. In Standards IEEE Std C57.154 and IEC 60076-14, the temperature limit of natural ester transformers is 15 °C higher than that of mineral oil transformers, which is the primary reason why natural esters can still meet temperature limits even under extreme high-temperature conditions. However, whether there are insulation defects due to the overall temperature increase in natural ester transformers remains to be studied. For example, the temperature rise in natural esters may cause bubble effect with multiphysics fields (e.g. temperature field, electric field, etc.), which leads to subsequent insulation breakdown [27]. Meanwhile, it is worth further studying whether natural ester impregnated insulation paper increases the risk of thermal breakdown due to temperature rise. Currently, the related research is insufficient, which needs more relevant study in the future.

## 5. Conclusion

This study discussed the thermal characteristics of the transformer filled with natural ester (TFNE) at extreme ambient temperatures, and the transformer filled with mineral oil (TFMO) is used for comparison. The main conclusions are listed as follows:

(1) Compared to mineral oil, natural esters are more prone to causing localized high temperatures in transformer windings due to their viscosity-temperature characteristic. Interestingly, there is a similar change pattern between the viscosity difference (natural esters and mineral oils) and the temperature rise difference (the windings of TFNE and TFMO).

(2) At extremely high ambient temperature (52.2 ℃), the hot-spot temperature of the TFNE is below the temperature limit of 110 °C specified by the IEEE/IEC standard; however, the hot-spot temperature of the TFMO has exceeded the temperature limit of 95 °C and the overheated zone accounts for approximately 50 % of the total winding. Mineral oil will exceed the standard requirements when the ambient temperature exceeds 45 °C, which reflects the superiority of natural esters for use at high ambient temperatures.

(3) The hot-spot temperatures of TFNE and TFMO initially decrease and then increase with the increment of ambient temperature, and the minimum values are 80.9 °C and 65.4 °C, respectively, which appears at -10℃ ambient temperature. At this time, an increase or decrease in the ambient temperature will lead to an increase in the hot-spot temperature. In addition, the hot-spot temperatures of TFNE and TFMO are located at the same position, which are located in the upper 97 % (321mm) of low voltage winding 2.


## Acknowledgement

The authors thank the project supported by National Natural Science Foundation of China (No. 52207152), Natural Science Foundation of Hebei Province (No. E2024202006) and S&T Program of Hebei (21567605H) (Corresponding author: Dawei Feng).


## Nomenclayure

$T$ -the thermodynamic temperature, [K]

$AT$ -ambient temperature, [℃]

## References


[1] Zhang, Y. Y., *et al.*, Bubble formation and motion characteristics in the transformer oil-paper insulation system under the extremely inhomogeneous electric field, *IEEE Transations on Dielectrics Electrical Insulation,* 30(2023), 4, pp. 1752-1759

[2] Lyutikova, M. N., *et al.*, Mixed Insulating Liquids With Mineral Oil for High-Voltage Transformer Applications: A Review, *IEEE Transations on Dielectrics Electrical Insulation*, 29(2022), 2, pp. 454-461

[3] Reffas, A., *et al.*, Comparison of breakdown voltage of vegetable olive with mineral oil, natural and synthetic ester liquids under DC voltage, *IEEE Transations on Dielectrics Electrical Insulation*, 27(2020), 5, pp. 1691-1697

[4] Wang, Y. W., *et al.*, Insulation design analysis for natural ester oil power transformers, *Proceedings*, 2024 IEEE 14th International Conference on the Properties and Applications of Dielectric Materials (ICPADM), Phuket, Thailand, 2024, pp. 291-294

[5] Seddik, M. S., *et al.*, Thermal analysis of power transformer using 2d and 3d finite element method, *Energies*, 17(2024), 13, pp.3203

[6] Liao, C. B., *et al.*, 3-D Coupled Electromagnetic-Fluid-Thermal Analysis of Oil-Immersed Triangular Wound Core Transformer, *IEEE Transactions on Magnetics*, 50(2014), 11, pp. 1-4

[7] IEEE Guide for Loading Mineral-Oil-Immersed Transformers and Step-Voltage Regulators, IEEE Std C57.91, 2011

[8] Power Transformers-Part 7:Loading Guide for Mineral-Oil-Immersed Power Transformers, IEC 60076-7, 2018

[9] Melka, B., *et al.*, Effective cooling of a distribution transformer using biodegradable oils at different climate conditions, *IEEE Transations on Dielectrics Electrical Insulation*, 30(2023), 4, pp. 1557-1565

[10] Deng, Y.Q., *et al.*, A Method for Hot Spot Temperature Prediction of a 10 kV Oil-Immersed Transformer, *IEEE Access*, 7(2019), pp. 107380-107388

[11] Feng, X.Y., *et al.*, Magnetic-Thermal-Flow Field Coupling Simulation of Oil-Immersed Transformer, *IEEE Access*, 12(2024), pp. 65462-65470

[12] Chereches, N.-C., *et al.*, Numerical study of cooling solutions inside a power transformer, *Energy Procedia*, 112(2017), pp. 314-321

[13] Zhang,X., *et al.*,Temperature distribution evolution of transformer windings thermal defect and its identification method(in Chinese), *High Voltage Engineering*, 50(2024), 4, pp. 1548-1559

[14] Liu, X.T., *Detailed Explanation of Engineering Examples for Finite Element Analysis Using ANSYS Workbench*(in Chinese), Railway Publishing House, Beijing, China, 2017

[15] Cargill, FR3® fluid behavior in cold temperature environments, https://www.cargill.com

[16] Cargill, Cold start recommendations for FR3® fluid filled transformers,.https://www.cargill.com

[17] Mehta, D. M., *et al.*, A review on critical evaluation of natural ester vis-a-vis mineral oil insulating liquid for use in transformers: Part 1, *IEEE Transations on Dielectrics Electrical Insulation*, 23(2016), 2, pp. 873-880

[18] Bayrak, E., *et al.*, Numerical study on mechanisms underlying the heat transfer enhancement of upward supercritical CO2 flow at low Reynolds numbers near the pseudo-critical region through a microtube, *International Communications in Heat and Mass Transfer*, 165 (2025)

[19] Ma, B., et al., A study on the optimization of cooling performance for oil-immersed transformers in high temperature environments utilizing response surface methodology, *Case Studies in Thermal Engineering*, 63(2024)

[20] Torriano, F., et al., Numerical and experimental thermofluidic investigation of different disc-type power transformer winding arrangements, *International Journal of Heat and Fluid Flow,* 69(2018)

[21] Dorella, J. J., et al., Enhancing heat transfer in power transformer radiators via thermo-fluid dynamic analysis with periodic thermal boundary conditions, *International Journal of Heat and Mass Transfer*, 222(2024)

[22] IEEE Standard for Liquid-Immersed Transformers Designed to Operate at Temperatures Above Conventional Limits Using High- Temperature Insulation Systems, IEEE Std C57.154, 202

[23] IEEE Standard for Test Procedure for Thermal Evaluation of Insulation Systems for Liquid-Immersed Distribution, Power, and Regulating Transformers, IEEE Std C57.100, 2022

[24] IEEE Standard for General Requirements for Liquid-Immersed Distribution, Power, and Regulating Transformers, IEEE Std C57.12.00, 2021

[25] IEEE Guide for the Application of High-Temperature Insulation Materials in Liquid-Immersed Distribution, Power, and Regulating Transformers, IEEE Std 1276, 2020

[26] Wang, Y. M., *et al*., Production pattern of furfural in esters-immersed paper and aging evaluation methods, *IEEE Transations on Dielectrics Electrical Insulation,* 2024

[27] Mo, S., *et al*., Effect of bubble flow on partial discharge under non-uniform AC electric fields in FC-72, *IEEE Transations on Dielectrics Electrical Insulation*, 27(2020), 4, pp. 1059 – 1067

Paper submitted: 26.04.2025
Paper revised: 21.05.2025
Paper accepted: 29.05.2025